



^{58}Ni as an Electron Diffraction Grating with ^{48}Ca as an Inert Core

Ali A. Mohammed ^{1*}  and Firas Z. Majeed ² 

^{1,2} Department of Physics, College of Science, University of Baghdad, Baghdad, Iraq.

*Corresponding Author.

Received: 24 May 2024

Accepted: 29 August 2024

Published: 20 April 2025

doi.org/10.30526/38.2.4005

Abstract

The configurations of the nuclear shell model were employed to study and inspect the form factor of a scattering electron in the ^{58}Ni nucleus. The wave function of the model space was obtained through the (fp-orbits) and (fpd6) effective interactions within the model space by utilizing the Harmonic Oscillator wave functions as a single particle's wave function. In the (fp-LS) shell, the correction for the main calculations of model space was performed by the 1st-order perturbation theory to estimate the effects of core polarization with the ($2\hbar\omega$) energy of excitation that has been carried out. Core polarization combined the model space with the discarded space (higher configuration core). Via model space, the interaction of effective (M3Y-P2) for linking the active particles of a model space with the particle-hole pair. The interaction of two bodies of Michigan 3-range Yukawa (M3Y) was used as a residual interaction for calculating the matrix elements of core polarization. Eventually, form factor theoretical results and the available experimental results were compared.

Keywords: Electron scattering, Shell model, Nickel-58, M3Y interaction.

1. Introduction

The scattering of electrons is a successful approach for looking into the structure and properties of nuclei (targets) (1). Elastic scattering for electrons is a technique in which the nucleus remains in its initial (ground) condition both before and after the scattering process. The spatial change in the nucleus's direction is denoted as the hole process. When the target persists in its ground state, its kinetic energy is altered as it merely absorbs the recoil momentum. Elastic scattering of electrons is very useful where it provides information, between other components, about the potential (target nucleus, projectile), which is important to give accurate computations of non-elastic processes theoretically and present an effective experimental instrument for comprehending the distributions of charge, transition probabilities, and radii (2). Information regarding the properties of isolated particles and the distribution of nuclear charge and nuclear wave functions has been obtained through longitudinal scattering of electron form factors. The longitudinal scattering of electron form factors has provided information regarding individual nucleons, in contrast to the proton-sensitive charge scattering (3). ^{48}Ni is the core nucleus in which the radius is measured, for ^{58}Ni it is the most essential nuclear system since it serves as the foundation for microscopic descriptions of nuclei (3).



The Fourier transform of the spatial charge distribution is represented by the form factor $\rho(r)$. This gives researchers a strong tool for determining the nuclei's spatial charge extent and shape. The form factor is acquired by comparing the measured cross-section to the Mott cross-section (1), which is dependent on Charge dispersion and magnetization in the target nucleus. Form factors can be experimentally determined by calculating the energy of incident and scattered electrons, as well as the scattering angle, as a function of momentum transfer (q) (2). The form factors of elastic magnetic electron scattering in ^{41}Ca have been studied. The $[1f_{7/2}]$ subshell had been employed to be a model space with one neutron. To achieve the vectors of model space for the form factors ($M1$, $M3$, $M5$, $M7$, and total), the Millinar, Baymann, and Zamick effective interaction (F7MBZ) for $[1f_{7/2}]$ was utilized as an effective interaction of model space. For the spaces (core and higher configuration orbits), which are the discarded space, the 1st Order perturbation theory relates the pair of particle-hole with $2\hbar\omega$ energy of excitation within the form factors calculations about the density dependence realistic (M3Y) interaction to be an interaction of core polarization with modern fitting parameters consists of five sets (4). The elastic scattering of the electron form factors of certain fp shell nuclei was analyzed by utilizing the fp shell as a model space and the effective (gxpfl) interaction within the model space to generate the wave functions.

The calculations included the core and higher configuration orbits as primary adjustments through the core polarization effect. The (M3Y-P0) residual interaction was used to link the pair of particles and holes within the space of models with the energy of excitation of $2\hbar\omega$. The available experimental data was compared with the theoretical conclusions (5). The frozen orbital method was utilized to compute the magnetic dipole moment in ^{50}Ti using the model of the nuclear shell for an excited state with $E_x = 10.23$ MeV, commonly referred to as the "mystery case." Various optional choices were considered, including core polarization interaction, restricted occupation, and effective interaction (6, 7). By coupling the model space's active particles with the pair (particle-hole), the disregarded (discarded) space (higher configuration core) was introduced via the influence of core polarization in a realistic interaction with effective M3y P2 (7). As a model space, the single orbit $1f_{7/2}$ was selected. With applying modern effective (M3Y) realistic interaction of (nucleon-nucleon) combined by two different groups of optimal parameters for fitting (Paris fitting (M3Y-P0), Ried fitting (M3Y-P1)), and the residual interactions (MSDI) were considered in the computation of effects by the polarization of the core in the longitudinal inelastic scattering of electron C6 form factor of Ti-50.

This was done within the 1st order of the theory of perturbation framework, coupling the core orbits to higher configurations with $2\hbar\omega$ excitation energy at normal transition through model space. Wave functions Harmonic oscillators (H.O) were utilized to be individual particle wave functions inside the $1f_{7/2}$ orbital (8). All of these data were compared to the experiment data. To investigate the effects of magnetic field form factors on individual and total multipole moments of electron scattering, a successful model based on the nuclear configurations of the shell model was modified. The eliminated space (higher configuration + core) was integrated into the model via the L-S shell, and an effective (M3Y P2) interaction was established between the moving particles in the spouse (p-h) and model space. As interaction residues, the two-body interactions M3Y were utilized in the computation of the matrix elements of core polarizability. A comparison is made between the form factor of the theoretical result and the experimental data (9, 10). When measuring energy levels and model space vectors, the shell theory approach with the model space and discarded spaces is successful and highly accurate (11–15).

2. Materials and Methods

Matrix elements that have been reduced from single-particle for the operator of electron scattering \hat{T}_A^η is defined by multiplying the product elements of the single-particle transition matrix (OBDM) by the matrix elements ($\langle\alpha||\hat{T}_A^\eta||\beta\rangle$), which are given by (1, 11, 12):

$$\begin{aligned} & \langle\Gamma_f||\hat{T}_A^\eta||\Gamma_i\rangle \\ &= \sum_{\alpha,\beta} OBDM(\Gamma_i, \Gamma_f, \alpha, \beta) \langle\alpha||\hat{T}_A^\eta||\beta\rangle \end{aligned} \quad (1)$$

Where (β, α) represent final and initial states of single particles, respectively (Isospin is incorporated). Both of the states $|\Gamma_f\rangle$ and $|\Gamma_i\rangle$ denote the ultimate and initial states of the nucleus, and the multi-polarity is $(\Lambda = JT)$. For the scattering electron operator, the reduced many-particle matrix element is separated into two parts: the (Model space) matrix element and the (Core-polarization) matrix element. (11):

$$\begin{aligned} \langle\Gamma_i\rangle &= \langle\Gamma_f||\hat{T}_A^\eta||\Gamma_i\rangle_{MS} \\ &+ \langle\Gamma_f||\delta\hat{T}_A^\eta||\Gamma_i\rangle_{CP} \end{aligned} \quad (2)$$

Where:

$\langle\Gamma_f||\hat{T}_A^\eta||\Gamma_i\rangle_{MS}$ denotes the reduced matrix element of the model space.

$\langle\Gamma_f||\delta\hat{T}_A^\eta||\Gamma_i\rangle_{CP}$ denotes the reduced matrix element of core polarization.

$|\Gamma_i\rangle$ is the initial nucleus state.

$|\Gamma_f\rangle$ is the initial nucleus state.

The 1st-order perturbation theory states that elements of the matrix for the single-particle for the higher-energy configurations can be expressed (1):

$$\begin{aligned} & \langle\beta\rangle \\ &= \langle P \rangle + \langle Q \rangle \end{aligned} \quad (3)$$

V_{res} is the residual interaction between model space and core particles

$\langle Q \rangle$ is the projection-out operator, $(H^{(0)})$ is the zeroth order Hamiltonian, and (E) is the energy eigenvalue.

The energies of a single particle are calculated according to (11- 17):

With:

$$\begin{aligned} e_{nlj} &= \left(2n + l - \frac{1}{2} \right) \hbar \\ &+ \begin{cases} -\frac{1}{2} (l+1) \langle f(r) \rangle_{nl} & \text{for } j = l - \frac{1}{2} \\ \frac{1}{2} l \langle f(r) \rangle_{nl} & \text{for } j = l + \frac{1}{2} \end{cases} \end{aligned} \quad (4)$$

$$\begin{aligned} & \langle f(r) \rangle_{nl} \\ & \approx -20A^{-\frac{2}{3}} \text{ MeV} \end{aligned} \quad (5)$$

$$\begin{aligned} & \hbar\omega \\ &= 45A^{-\frac{1}{3}} - 25A^{-\frac{2}{3}} \end{aligned} \quad (6)$$

$\langle f(r) \rangle_{nl}$ is the averaged surface energy, (A) is the mass number, (ω) is the angular frequency, (n) represents the principal quantum number, (j) is total spin, and (l) is the orbital angular momentum quantum number. The reduced elements of the single particle matrix in both isospin

and spin are represented in terms of the single-particle elements of the matrix that have only been reduced in spin (1-3,11,12),

$$\begin{aligned} & \langle \alpha || \hat{T}_A^\eta || \beta \rangle \\ &= \sqrt{\frac{2T+1}{2}} \sum_{t_z} I_T(t_z) \langle j_1 \rangle \end{aligned} \quad (7)$$

With

$$\begin{aligned} & \sum_{t_z} I_T(t_z) \\ &= \begin{cases} 1 & \text{for } T = 0 \\ (-1)^{\frac{1}{2}-t_z} & \text{for } T = 1 \end{cases} \end{aligned} \quad (8)$$

t_z is the isospin projection quantum number where $[t_z = \frac{1}{2}]$ for proton and $[t_z = -\frac{1}{2}]$ for neutron.

Regarding the residual interaction, the matrix consists of two-body elements. $\langle \beta \alpha_2 \rangle_T$ and $\langle \beta \alpha_1 \rangle_T$ $\alpha, \alpha_1, \alpha_2, \beta$ are the states of the interacting single particles (presented in the equation (3)). For the residual interaction of the two, the interaction (M3Y) is adopted (11, 20-27). Form factors of scattering electrons, which include momentum transfer (q) and angular momentum (J) between initial and final nuclear shell model states of spin ($J_{i,f}$) and isospin ($T_{i,f}$) are (11, 21-23, 28-30):

$$\begin{aligned} |F_f^\eta(q)|^2 &= \frac{4\pi}{Z^2(2J_i+1)} \\ &\times \left| \sum_{T=0,1} (-1)^{T_f-T_{z_f}} \left(T_f \ T \ T_i \ -T_{z_f} \ M_T \ T_{z_i} \right) \langle J_f T_f || \hat{T}_{JT}^\eta || J_i T_i \rangle \right|^2 \\ &\times |F_{c.m}(q)|^2 |F_{f.s}(q)|^2 \end{aligned} \quad (9)$$

3. Results and Discussion

Inelastic scattering of electron form factor for ^{58}Ni with ^{48}Ca as inert core, the (fp) shell was used as a model space in which fpd6 was employed to construct the model space factor, considering the potential of a Harmonic oscillator for a single particle. All the theories were investigated utilizing nuclear shell theory. Core polarization impact with modern effective residual (M3Y-p2) interaction is utilized for coupling particle-hole pairs within the model space. The wave function for the (fp) shell model space and the (OBDM) are computed using the (OXBASH) code. The form factor of longitudinal inelastic electron scattering is valuable for determining the charge multipole moment of an atom in its excited state. It also assists in calculating the magnetic moment and probability for each multipole moment. From **Figure 1**, which represents the (C0 form factor), the contributions are noticeable, particularly at momentum transfer ($q < 1.5 \text{ fm}^{-1}$), which is considered low, with the main contribution being dominant over the model space. The values of the total form factor indicate that the core and model space contributions interfere destructively, causing the diffraction minima to shift as the momentum transfer increases. In another Figure, the behavior of the (C2) form factor is nearly identical to the experimental data. However, for the second portion in **Figure 2**, the analysis of the data shows that the main effect on the first lobe comes from the model space rather than the core component. Notably, core orbits solely determine the overall form factor, while the

contribution from the model space disappears. In **Figure 3**, (E2) Form factor is displayed. The model space has a clear and ready contribution. The core part is the second space originating at ($q=0 \text{ fm}^{-1}$ to $q=3.5 \text{ fm}^{-1}$), with one lobe making the nucleus widely spreader in momentum space and behaving as a diffraction grating. The model needs more corrections to give the calculation accurate results. **Figure 4** demonstrates the (M3 form factor), where the dominating model space is. The core component ranges between [$q=0 \text{ fm}^{-1}$ to $q=3.5 \text{ fm}^{-1}$], with one lobe causing the nucleus to be widely dispersed in momentum space and function as a diffraction grating. The model requires additional adjustments to produce precise calculations.

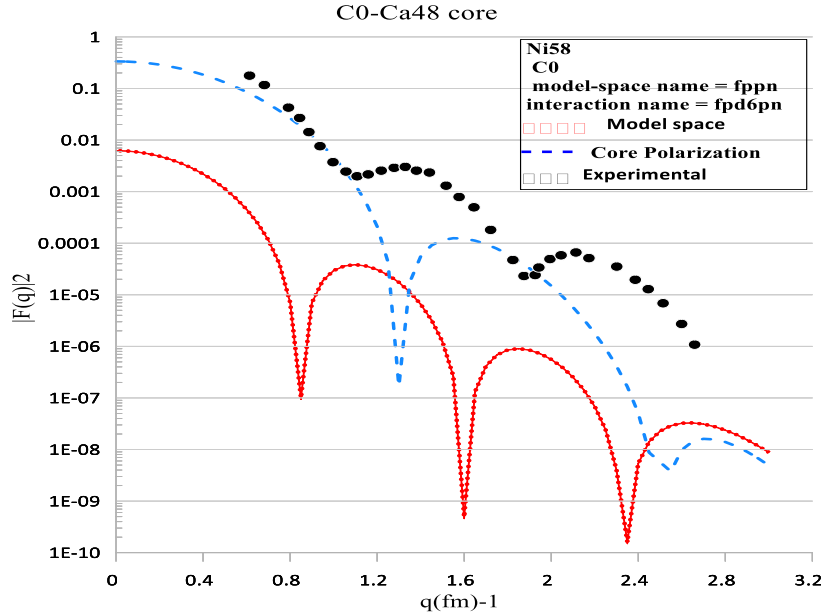


Figure 1. C0 Charge form factors.

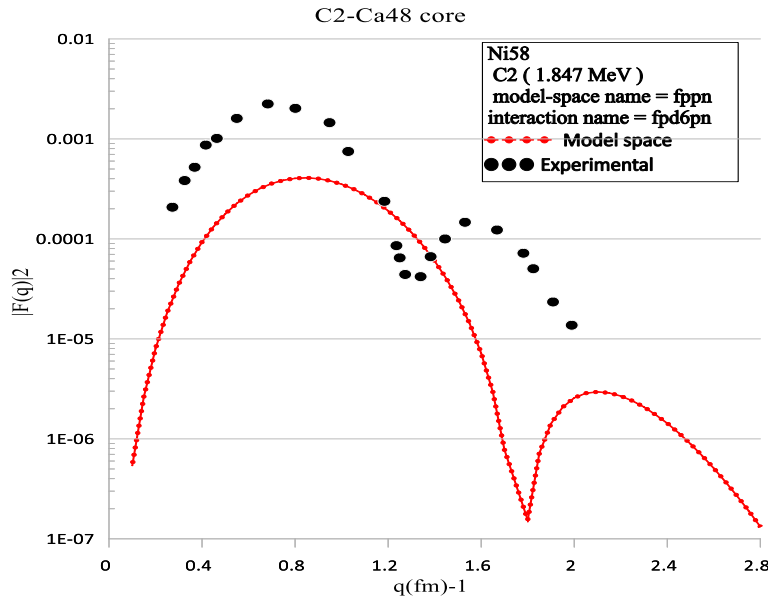


Figure 2. The Total C2 form factors at $E_x=1.847 \text{ MeV}$.

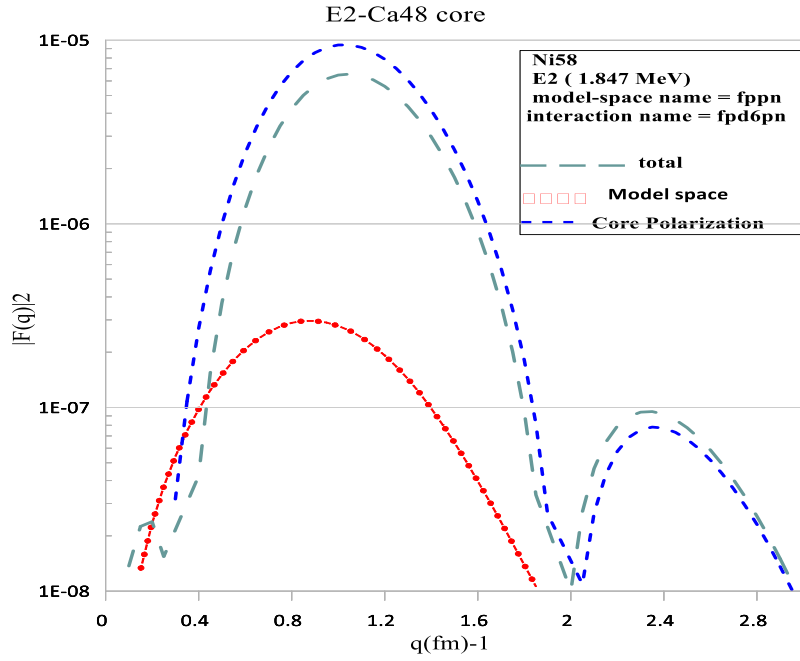


Figure 3. The Total E4 form factors at $E_x=1.847$ MeV.

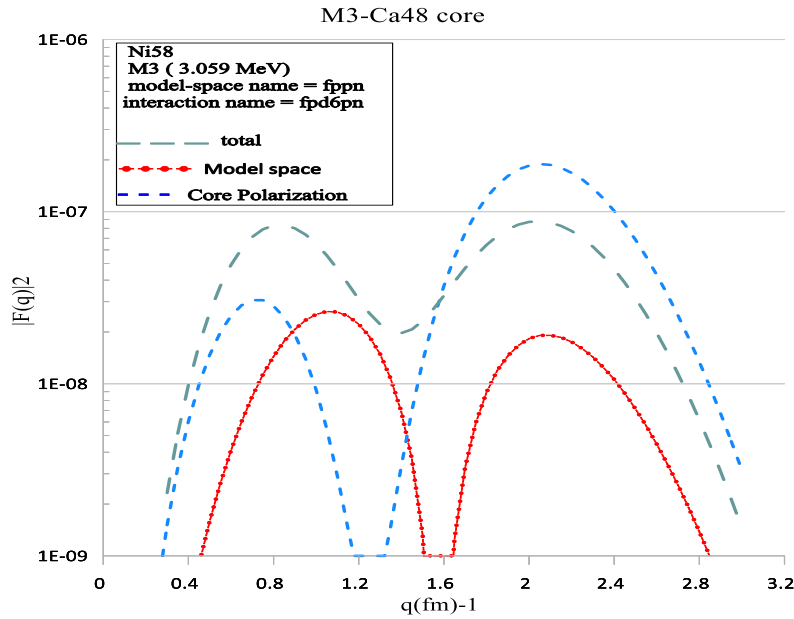


Figure 4. The Total M3 form factors at $E_x=3.059$ MeV.

4. Conclusion

The technique of electron scattering form factors is still effective and valid to measure and interpret the structure and properties of nuclear observables by utilizing the nuclear shell theory, which involves interactions and transitions. ^{58}Ni is a good example of a (fp) shell model space nucleus to be tested to understand the N-N interaction, and the form factor results reflect the efficiency of ^{48}Ca as an inert core.

Acknowledgment

The researchers are very grateful to Dr. Boyed A. Brown for his code (OXBASH) and also to Dr. Read A. Radhi for the Fortran code of form factors and the Fortran code of residual interaction.

Conflict of Interest

There is no conflict of interest in this article.

Funding

The article was done depending on self-fund and no establishments supplied us.

Ethical Clearance

The work and calculations were accomplished using the OXBASH nuclear shell model code 2005 and the Fortran power station code of Prof. Dr. Read A. Radhi.

References

1. Mott NF. An Introduction to Particle Physics and the Standard Model. Soci Ser. 1929;A124:425.
2. Donnelly TW, Sick I.). Elastic magnetic electron scattering from nuclei. Rev Mod Phys. 1984;56:461. <https://doi.org/10.1103/RevModPhys.56.461>
3. Majeed FZ, Hmood FM. Inelastic longitudinal electron scattering C2 form factors in 58Ni. Iraqi J Phys. 2016;14(29):15-26. <https://doi.org/10.30723/ijp.v14i29.216>
4. Radhi RA, Majeed FZ. Elastic magnetic electron scattering form factor in Ca-41 (M3Y fitting parameters consideration). Iraqi J Phys. 2010;8(13):18-27. <https://doi.org/10.30723/itr.v14i29.205>
5. Majeed FZ. M3Y-P0 as a residual interaction to study elastic magnetic electron scattering form factors for Ca-41. Al-Nahrain J Sci. 2013;16(3):141-147. <https://anjs.edu.iq/index.php/anjs/article/view/598/535>.
6. Majeed FZ, Qassim AA. 1f7/2 1d3/2 model space and inelastic longitudinal C6 electron scattering form factors in 50Ti (residual interactions consideration). Iraqi J Sci. 2012;53(4):807-813. <https://doi.org/10.24996/236601>.
7. Majeed FZ, Mashaan SS. Inelastic longitudinal electron scattering C2 form factors in 48Ca nucleus by using sigma meson as a residual interaction. Iraqi J Sci. 2014;55(1):151-160. <https://ijs.uobaghdad.edu.iq/index.php/eijs/article/view/11939>.
8. Majeed FZN, Albana'a MA, Qassim AA. Inelastic longitudinal C6 electron scattering form factors in 50Ti (residual interactions consideration). Iraqi J Sci. 2012;53(3):564-572. <https://doi.org/10.13140/RG.2.2.12919.14243>.
9. Hussien RM, Majeed FZ. The effective M3Y residual interaction in nuclear diffraction grating of electrons for Ca41. Baghdad Sci J. 2022;19(6):1393-1398. <https://doi.org/10.21123/bsj.2022.6776>.
10. Falih R, Majeed FZ. Gogny interaction and nuclear charge distribution in 48Ca nucleus. Baghdad Sci J. 2023;20(3):815-824. <https://doi.org/10.21123/bsj.2022.7007>.
11. Radhi RA, Bouchebak A. Microscopic calculations of C2 and C4 form factors in sd-shell nuclei. Nucl Phys. 2003;A716:87. [https://doi.org/10.1016/S0375-9474\(02\)01335-0](https://doi.org/10.1016/S0375-9474(02)01335-0).
12. Brussaard PJ, Glademans PWM. Shell-model application in nuclear spectroscopy. Amsterdam: North-Holland Publishing Company; 1977. [https://doi.org/10.1016/sr34-23\(3\)0123](https://doi.org/10.1016/sr34-23(3)0123).
13. Hasan MK, Majeed FZ. FP shell effective interactions and nuclear shell structure of 44Sc. East Eur J Phys. 2023;1:89-93. <https://doi.org/10.26565/2312-4334-2023-1-10>.
14. Kadhum HA, Majeed FZ. Nuclear energy levels scheme of 46Cr using FPD6, FPY, and KB3G interactions. East Eur J Phys. 2023;3:187-191. <https://doi.org/10.26565/2312-4334-2023-3-15>.
15. Hasan MK, Majeed FZ. Nuclear energy levels in 44Ca using FPD6pn interaction. East Eur J Phys. 2023;1:69-74. <https://doi.org/10.26565/2312-4334-2023-1-18>.
16. Yokoyama A. Inelastic longitudinal C6 electron scattering form factors in 50Ti. J Phys Conf. 2005;20:143-146. <https://doi.org/10.13140/RG.2.2.12919.14243>.

17. Majeed FZ. Core polarization effects on electron scattering form factors for some fp-shell nuclei. Doctoral dissertation, University of Baghdad, Department of Physics, College of Science, Baghdad, Iraq; 2009:114-139. <https://doi.org/10.24996/Iraqijournalofscience.v5i3.12760>.
18. Elliott P, Skyrme THR. An effective interaction for inelastic scattering derived from the nucleon potential. Proc Roy Soc. 1955;A323:561-576. [https://doi.org/10.1016/0375-9474\(83\)90487-6](https://doi.org/10.1016/0375-9474(83)90487-6).
19. Yeslam HA. Core-polarization effects for electron scattering form factors in some sd-shell nuclei. Doctoral dissertation, University of Baghdad, Department of Physics, College of Science, Baghdad, Iraq; 2005:56-70.
20. Sakakura M, Arima A, Sebe T. Application to electron scattering of center-of-mass effects in the nuclear shell model. Phys Lett. 1976;61B:335-351. [https://doi.org/10.1016/0370-2693\(79\)90909-2](https://doi.org/10.1016/0370-2693(79)90909-2).
21. Nakada H, Sato M. Hartree-Fock approach to nuclear matter and finite nuclei with M3Y-type nucleon-nucleon interactions. Nucl Phys. 2002;A699:511-525. <https://doi.org/10.48550/arXiv.nucl-th/0304021>.
22. Brown BA, Etchegoyen A, Godwin NS, Rae WDM, Richter WA, Ormand WE, et al. Nuclear shell model code. MSU-NSCL report number 1289; 2005. <https://doi.org/10.1016/j.nds.2014.07.022>.
23. Heisenberg J, McCarthy JS, Sick I. Inelastic electron scattering from several Ca, Ti, and Fe isotopes. Nucl Phys. 1971;A164:353-374. [https://doi.org/10.1016/0375-9474\(71\)90219](https://doi.org/10.1016/0375-9474(71)90219).
24. Edmonds R. Angular Momentum in Quantum Mechanics. 3rd ed. Princeton: Princeton University Press; 1974. p. 70-113. <https://doi.org/10.1515/9781400884186>.
25. Walecka JD. Electron scattering for nuclear and nucleon structure. Cambridge: Cambridge Monographs on Physics, Nuclear Physics and Cosmology; 2004. p. 12-42. <https://doi.org/10.1017/9781009290616>.
26. Haxel O, Jensen JHD, Suess HE. On the "Magic Numbers" in nuclear structure. Phys Rev. 1949;75:1766-1780. <https://doi.org/10.1103/PhysRev.75.1766.2>.
27. Berstch G, Borysowicz J, McManus H, Love WG. An effective interaction for inelastic scattering derived from the Paris potential. Nucl Phys. 1977;A284:399-418. [https://doi.org/10.1016/0375-9474\(83\)90487-6](https://doi.org/10.1016/0375-9474(83)90487-6).
28. Goriely S, Tondeur F, Pearson JM. Atomic and nuclear datasheet. At Data Nucl Data Sheets. 2001;77:311-420. <https://doi.org/10.1006/adnd.2000.0857>.
29. Lalazissis GA, Koonig J, Ring P. Central and noncentral components of the effective sd-shell interaction. Phys Rev. 1997;C55:540-567. <https://doi.org/10.1103/PhysRevC.15.1483>.
30. Khoa DT, Von Oertzen W, Ogloblin AA. Study of the equation of state for asymmetric nuclear matter and interaction potential between neutron-rich nuclei using the density-dependent M3Y interaction. Nucl Phys. 1996;A602:98-213. [https://doi.org/10.1016/0375-9474\(96\)00091-7](https://doi.org/10.1016/0375-9474(96)00091-7)